

Coalescing Majorana edge modes in non-Hermitian \mathcal{PT} -symmetric Kitaev chain

C. Li, L. Jin and Z. Song*

School of Physics, Nankai University, Tianjin 300071, China

A single unit cell contains all the information about the bulk system, including the topological feature. The topological invariant can be extracted from a finite system, which consists of several unit cells under certain environment, such as a non-Hermitian external field. We investigate a non-Hermitian finite-size Kitaev chain with \mathcal{PT} -symmetric chemical potentials. Exact solution at the symmetric point shows that Majorana edge modes can emerge as the coalescing states at exceptional points and \mathcal{PT} symmetry breaking states. The coalescing zero mode is the finite-size projection of the conventional degenerate zero modes in a Hermitian infinite system with the open boundary condition. It indicates a variant of the bulk-edge correspondence: The number of Majorana edge modes in a finite non-Hermitian system can be the topological invariant to identify the topological phase of the corresponding bulk Hermitian system.

I. INTRODUCTION

The discovery of topological matter which exhibits topological properties in the band structure has opened a growing research field [1–5]. A particularly important concept is the bulk-edge correspondence, which indicates that, a nontrivial topological invariant in the bulk indicates localized edge modes that only appear in the presence of the open boundary in the thermodynamic limit. In general, a bulk system is constructed by stacking a great many copies of a single original unit cell in an array. In this sense, a single unit cell contains all the information about the bulk system, including the topological feature. Then the topological invariant can be, in principle, extracted from a finite system, which consists of several unit cells under certain environment, such as a non-Hermitian external field. In fact, the original bulk-edge correspondence is an example in this context: The open boundary can be technically regarded as one of the extreme cases of adding local impurity on the bulk, that breaks the translational symmetry. On the other hand, it has been shown that a finite system with imaginary ending potentials can share the common eigenstates with an infinite system [6]. It implies that a finite non-Hermitian system may retain some of characteristics, such as zero-energy modes of an infinite Hermitian system. An interesting question is whether there is a generalization of the bulk-edge correspondence to non-Hermitian systems which arises from the imaginary impurity.

In this work, we investigate a non-Hermitian finite-size Kitaev chain with parity-time (\mathcal{PT}) symmetric chemical potentials. We demonstrate that the key to retrieve the Majorana zero mode from a small system is a pair of specific imaginary chemical potentials, under which the coalescing zero mode shares the identical pattern with that of the conventional zero mode in the thermodynamic limit. The coalescing zero mode in a finite-size non-Hermitian system can be directly obtained from the projection of the conventional degenerate zero modes in

a Hermitian infinite system. Exact solution also shows the existence of Majorana edge modes, which emerge as a pair of \mathcal{PT} symmetry breaking states with imaginary eigenvalues. It indicates a variant of the bulk-edge correspondence: The number of Majorana edge modes in a finite-size non-Hermitian system can be the topological invariant to identify the topological phase of the corresponding bulk Hermitian system.

The remainder of this paper is organized as follows. In Sec. II, we present the Hamiltonian of the Kitaev ring with two impurities. In Sec. III the corresponding Majorana representation of the model with \mathcal{PT} -symmetric chemical potentials is given. Sec. IV devotes to the investigation of Majorana bound states at the symmetric point. In Sec. V, we reveal the link between the coalescing zero mode and the Hermitian one. Finally, we present a summary and discussion in Sec. VI.

II. MODEL HAMILTONIANS

We consider a one-dimensional Kitaev model with two impurities. The Hamiltonian of the tight-binding model takes the following form

$$\begin{aligned} H &= H_0 + H_{\text{im}}, \\ H_0 &= - \sum_{j=1}^N (tc_j^\dagger c_{j+1} + \Delta c_j^\dagger c_{j+1}^\dagger + \text{H.c.}) - \mu \sum_{j=1}^N (1 - 2n_j), \\ H_{\text{im}} &= (\mu - \mu_L)(1 - 2n_1) + (\mu - \mu_R)(1 - 2n_{N/2+1}), \end{aligned} \quad (1)$$

where j is the coordinate of lattice sites and c_j is the fermion annihilation operator at site j . H_0 is employed to depict p -wave superconductors. The hopping between (pair operator of) neighboring sites is described by the hopping amplitude t (the real order parameter Δ). The last term in H_0 gives the chemical potential. Imposing the periodic boundary condition $c_1 \equiv c_{N+1}$, the Hamiltonian H_0 can be exactly diagonalized and the topological invariant can be obtained in various parameter regions. It provides well-known example of systems with the bulk-edge correspondence when the open boundary condition is imposed. It turns out that a sufficient long chain has

* songtc@nankai.edu.cn

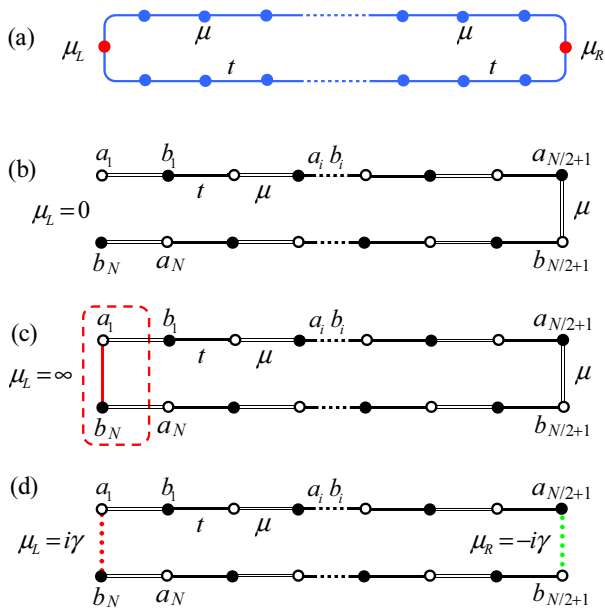


FIG. 1. (Color online) Schematic illustrations for edge modes in the Majorana Hamiltonian from Eq. (1), induced by impurities embedded in a Kitaev ring. (a) N -site Kitaev ring with uniform chemical potential μ and hopping amplitude (pairing amplitude) t . Two impurities are located at sites 1 and $N/2 + 1$, in terms of specific values of chemical potentials μ_L and μ_R , respectively. The corresponding Majorana lattice is a $2N$ -site dimerized ring with staggered hopping strengths t (single line) and μ (double line), which contains two specific dimers with hopping amplitudes μ_L and μ_R . We focus on three cases: (b) $\mu_L = 0$, $\mu_R = \mu$, the lattice becomes a standard $2N$ -site SSH chain, which possesses edge modes for $\mu > 1$. (c) $\mu_L = \infty$, $\mu_R = \mu$, the dimer (circled by the dashed red line) is adiabatic eliminated, and then the lattice becomes a standard $2(N - 1)$ SSH chain, which possesses edge modes for $\mu < 1$. For infinite N , the conclusions for cases (b) and (c) can be regarded as the extension of original bulk-edge correspondence. (d) $\mu_L = -\mu_R = i\gamma$, it is \mathcal{PT} symmetric. For finite N , it has two coalescing zero modes for $\mu > 1$, while two degenerate zero modes and two imaginary-energy modes for $\mu < 1$. All these modes exhibit evanescent wave behavior. The number of edge modes for finite system matches the topological invariant of the bulk. It indicates that bulk-edge correspondence can be extended to the non-Hermitian regime.

Majorana modes at its two ends [7]. A number of experimental realizations of p -wave superconductors have found evidence for such Majorana modes [8–12]. Term H_{im} represents two impurities on the two symmetrical sites. The impurities are described in terms of specific values of chemical potentials μ_L and μ_R . We note that taking $\mu_L = 0$ or $\pm\infty$, and $\mu_R = \mu$, it corresponds to the open Majorana chains with different edges (see Fig. 1). It is an alternative representation of bulk-boundary correspondence. In this context, the real value of $\mu_{L,R}$ requires an infinite system. In this work, we consider imaginary value of $\mu_{L,R}$. In contrast to previous studies based on Hermitian chains in the thermodynamic limit,

we focus on the Kitaev model on a finite lattice system. This is motivated by the desire to get a clear physical picture of the edge mode through the investigation of a small system. We first study the present model from the description in terms of Majorana fermions. We will show that the evident indicator for phase diagram does not require infinite system.

III. MAJORANA REPRESENTATION

In the following, the impurity is taken as \mathcal{PT} symmetric with $\mu_L = i\gamma$ and $\mu_R = -i\gamma$. Note that the Hamiltonian H is not \mathcal{PT} symmetric unless Δ is pure imaginary. Here the space-reflection operator, or the parity operator \mathcal{P} and the time-reversal operator \mathcal{T} , are defined as

$$\mathcal{P}c_l^\dagger\mathcal{P} = c_{N+1-l}^\dagger, \mathcal{T}i\mathcal{T} = -i. \quad (2)$$

Nevertheless, we will see that the core matrix in the Majorana fermion representation is \mathcal{PT} symmetric, which ensures the system is pseudo-Hermitian.

We introduce Majorana fermion operators

$$a_j = c_j^\dagger + c_j, b_j = -i(c_j^\dagger - c_j), \quad (3)$$

which satisfy the relations

$$\begin{aligned} \{a_j, a_{j'}\} &= 2\delta_{jj'}, \{b_j, b_{j'}\} = 2\delta_{jj'} \\ \{a_j, b_{j'}\} &= 0, a_j^2 = b_j^2 = 1. \end{aligned} \quad (4)$$

Then the Majorana representation of the Hamiltonian is

$$\begin{aligned} \mathcal{H} &= -\frac{i}{4} \sum_{j=1}^N [(t + \Delta) b_j a_{j+1} + (t - \Delta) b_{j+1} a_j] \\ &\quad - \frac{i}{2} \sum_{j \neq 1, N/2+1}^N \mu a_j b_j + \text{H.c.} \\ &\quad + \frac{\gamma}{2} (a_1 b_1 - a_{N/2+1} b_{N/2+1} - \text{H.c.}). \end{aligned} \quad (5)$$

The diagonalization of H is directly related to a model of two coupled SSH chain, which was systematically studied in Ref. [13].

IV. EDGE MODES

Majorana edge mode plays an important role in the characterization of the topological feature of matter, such as the bulk-edge correspondence. The Majorana particle is localized at two ends. Since the pattern of the zero mode is exponentially decaying, the bound Majorana particle must require infinite chain condition. Therefore the conventional zero mode cannot exist in a Hermitian system except for some trivial cases [14]. In this paper, we focus on a finite-size non-Hermitian system and we

define the edge mode by the evanescent wave characterization.

We consider a Kitaev ring at the symmetric point $\Delta = t$. We write down the Hamiltonian as the form

$$\mathcal{H} = \psi^T h \psi, \quad (6)$$

in the basis $\psi^T = (a_1, b_1, a_2, b_2, a_3, b_3, \dots, a_N, b_N)$, where h represents a $2N \times 2N$ matrix. Here matrix h is explicitly written as

$$h = -\frac{i}{2} \left(\sum_{l=1}^N t |2l\rangle \langle 2l+1| + \sum_{l \neq 1, N/2+1}^N \mu |2l-1\rangle \langle 2l| + \text{H.c.} \right) + \frac{\gamma}{2} (|1\rangle \langle 2| - |N+1\rangle \langle N+2| - \text{H.c.}) \quad (7)$$

where basis $\{|j\rangle, j \in [1, 2N]\}$ is an orthonormal complete set, $\langle j | j' \rangle = \delta_{jj'}$. By taking the linear transformation

$$\begin{cases} |\sigma, 2l-1\rangle = \frac{e^{-i\pi/4}}{2} (|2l\rangle + i\sigma |2N+3-2l\rangle) \\ |\sigma, 2l\rangle = \frac{e^{i\pi/4}}{2} (|2l+1\rangle - i\sigma |2N+2-2l\rangle) \end{cases} \quad (8)$$

with $l \in [1, N/2]$ and $\sigma = \pm$, we can express matrix h as $h = h_+ + h_-$ with

$$[h_+, h_-] = 0, \quad (9)$$

where

$$h_\sigma = t \sum_{l=1}^{N/2} |\sigma, 2l-1\rangle \langle \sigma, 2l| - \mu \sum_{j=1}^{N/2-1} |\sigma, 2l\rangle \langle \sigma, 2l+1| + \text{H.c.} + \sigma i \gamma (|\sigma, 1\rangle \langle \sigma, 1| - |\sigma, N\rangle \langle \sigma, N|). \quad (10)$$

Obviously, h_\pm describes two identical SSH chains with opposite imaginary ending potentials $\pm i\gamma$. It is a \mathcal{PT} symmetric system and has been studied in Refs. [15] for $\mu > t$ and the topological phase in the similar systems has been studied in Refs. [16]. It is shown that there is a single zero mode in such a finite degree of non-Hermiticity at the exceptional point (EP).

Now we concentrate on a single non-Hermitian SSH chain with the Hamiltonian

$$h_{\text{SSH}} = \sum_{l=1}^{N/2} |2l-1\rangle \langle 2l| - \sum_{l=1}^{N/2-1} \mu |2l\rangle \langle 2l+1| + \text{H.c.} + i\gamma (|1\rangle \langle 1| - |N\rangle \langle N|), \quad (11)$$

where we take $t = 1$ and $\mu > 0$ for the sake of simplicity. Note that h_{SSH} and h_{SSH}^\dagger represent h_+ and h_- , respectively. Here we redefine the space-reflection operator, or the parity operator \mathcal{P} in the space spanned by the complete set $\{|l\rangle\}$. The action \mathcal{P} on $|l\rangle$ is given by the equality

$$\mathcal{P} |l\rangle = |N+1-l\rangle. \quad (12)$$

Then we have $[h_{\text{SSH}}, \mathcal{PT}] = 0$, which implies that h_{SSH} is pseudo-Hermitian [17], i.e., h_{SSH} has either real spectrum

or its complex eigenvalues occur in complex conjugate pairs. On the transition from a pair of real levels to a complex conjugate pair, or EP, two levels coalesce to a single level. The key point of our approach is to link the zero-eigenvalue coalescing eigenvector to the conventional Majorana zero mode in the thermodynamic limit.

The Bethe ansatz wave function $|\psi_k\rangle = \sum_{l=1}^N f_l^k |l\rangle$ has the form

$$f_l^k = \begin{cases} A_k e^{ikl} + B_k e^{-ikl}, & l = 2j-1 \\ C_k e^{ikl} + D_k e^{-ikl}, & l = 2j \end{cases}, \quad (13)$$

where $j = 1, 2, \dots, N/2$. Following the derivation in the Appendix A, when the imaginary potential takes the value

$$\gamma = \mu^{1-N/2}, \quad (14)$$

there are three types of eigenvector $|\psi_k\rangle$, with the eigenvalue

$$\varepsilon_k = \pm \sqrt{1 + \mu^2 - \mu(e^{2ik} + e^{-2ik})}. \quad (15)$$

In general, the EP varies as the system size changes. In the present model, $\gamma = \mu^{1-N/2}$ is N dependent except when $\mu = 1$. It is reasonable that the system is always at the EP for any N . We note that in the case of $\mu = 1$, it reduces to a uniform chain with $\gamma = 1$, which was studied in Ref. [18]. The solutions for $\mu \neq 1$ is concluded as follows.

(i) Scattering vector with real eigenvalues: In this case, k is a real number, the eigenvalue is real. The energy gap has a lower bound

$$\Delta_{\text{Gap}} \geq 2|1 - \mu|, \quad (16)$$

which is crucial to protect the degenerate ground states of the original Kitaev model from decoherence.

(ii) Coalescing vector with zero eigenvalue: Here the wave vector is imaginary, $k = \pm \frac{i}{2} \ln \mu$. The eigenvector has the form

$$|\psi_{\text{zm}}\rangle = \Omega \sum_{j=1}^{N/2} (\mu^{1-j} |2j-1\rangle - i\mu^{j-N/2} |2j\rangle), \quad (17)$$

satisfying

$$h_{\text{SSH}} |\psi_{\text{zm}}\rangle = 0. \quad (18)$$

where $\Omega = \mu^{N/2-1} \sqrt{(1-\mu^2)/(2-2\mu^N)}$ is the Dirac normalizing constant. It is \mathcal{PT} symmetric and has a zero biorthogonal norm, indicating the coalescence of two levels. Actually, the zero-mode vector for h_{SSH}^\dagger can be constructed as

$$|\eta_{\text{zm}}\rangle = \Omega \sum_{j=1}^{N/2} (\mu^{1-j} |2j-1\rangle + i\mu^{j-N/2} |2j\rangle), \quad (19)$$

satisfying

$$h_{\text{SSH}}^\dagger |\eta_{\text{zm}}\rangle = 0. \quad (20)$$

TABLE I. For N -site system, $\gamma = \mu^{1-N/2}$, n_I is the number of imaginary levels, n_{EP} is the number of coalescing state, n_S is the number of real levels. We have $n_I + 2n_{EP} + n_S = N$.

μ	n_I	n_{EP}	n_S
$\mu > 1$	0	1	$N - 2$
$\mu < 1$	2	1	$N - 4$

On the other hand, it is easy to check

$$\langle \eta_{zm} | \psi_{zm} \rangle = 0, \quad (21)$$

and

$$|\eta_{zm}\rangle = i\mathcal{P} |\psi_{zm}\rangle \text{ or } |\eta_{zm}\rangle = (|\psi_{zm}\rangle)^*, \quad (22)$$

which indicate that the vector $|\psi_{zm}\rangle$ has a zero biorthogonal norm and the relations between two conjugate vectors. Based on these facts we conclude that the zero-mode vector $|\psi_{zm}\rangle$ is a coalescing vector for $\mu \neq 1$. The exact wave function of $|\psi_{zm}\rangle$ clearly indicates that it is a superposition of two parts with nonzero amplitudes only located at even or odd sites, respectively. We will show that vectors $|\eta_{zm}\rangle$ and $|\psi_{zm}\rangle$ have a close relation to the standard zero modes of a Hermitian chain in the thermodynamic limit.

(iii) Evanescent wave vector with imaginary eigenvalue: The derivation in the Appendix A shows that this kind of state only appears at $\mu < 1$. In this case, k is still imaginary. Since matrix h_{SSH} is pseudo-Hermitian, this type of eigenvector always appears in pair. The wave vector approximately takes

$$k = \pm i \frac{N-1}{2} \ln \mu \quad (23)$$

in large N or small μ and the wave function reads

$$|\psi_{IM}^\sigma\rangle \approx \frac{1}{2} [(1 + \sigma) |1\rangle + (1 - \sigma) |N\rangle], \quad (24)$$

satisfying

$$h_{SSH} |\psi_{IM}^\sigma\rangle = i\sigma |\varepsilon_{IM} | \psi_{IM}^\sigma\rangle. \quad (25)$$

with approximate eigenvalue

$$\varepsilon_{IM} \approx \pm i \mu^{1-N/2}, \quad (26)$$

We can see that the \mathcal{PT} symmetry is broken. Both the two vectors present evanescent wave and

$$|\psi_{IM}^\sigma\rangle = \mathcal{PT} |\psi_{IM}^{-\sigma}\rangle, \quad (27)$$

which indicates that $|\psi_{IM}^\pm\rangle$ are symmetry breaking. We summarize the solutions in Table I.

It is well known that the number of Majorana zero mode for an infinite Hermitian Kitaev chain with open

boundary conditions can be a topological invariant, referred as the bulk-edge correspondence. Similarly, the result in Table I indicates the number of Majorana edge modes in a finite non-Hermitian system can also be the topological invariant to identify the topological phase of the corresponding bulk Hermitian system. This can be regarded as a variant of the bulk-edge correspondence in the complex regime. Recently, non-Hermitian SSH chains were experimentally realized by coupled dielectric microwave resonators [19, 20] and photonic lattices [21, 22]. In Appendix B, we provide exact solutions for a 6-site system to demonstrate our main idea, which can be a protocol for the experimental investigation.

V. CONNECTION TO CONVENTIONAL ZERO MODE

In this section, we investigate the connection for the zero-mode states between the present non-Hermitian model and infinite Hermitian SSH chain. We consider h_{SSH} in the large N limit and analyze the solutions in the following two regions.

(i) In the case of $\mu > 1$, we have $\gamma = \mu^{1-N/2} \rightarrow 0$. Matrices h_{SSH} and h_{SSH}^\dagger become the same matrix of N -site single-particle Hermitian SSH chain with open boundary conditions. Two zero-mode wave functions $|\eta_{zm}\rangle$ and $|\psi_{zm}\rangle$ become two degenerate zero modes of the same Hermitian SSH chain. Remarkably, the Eq. (21) for characterizing the coalescing levels is nothing but the Dirac orthogonality of two degenerate zero modes. On the other hand, we note that the amplitudes in $|\eta_{zm}\rangle$ and $|\psi_{zm}\rangle$ are only determined by μ , independent of N . The coalescing zero mode is the finite-size projection of the conventional degenerate zero modes in a Hermitian infinite system with the open boundary condition. In this sense, the coalescing zero modes $|\eta_{zm}\rangle$ and $|\psi_{zm}\rangle$ for any small N carry the complete information of conventional zero modes for the SSH chain.

(ii) Now we turn to the case of $\mu < 1$. In contrast to the case (i), we have $\gamma = \mu^{1-N/2} \gg 1$. Therefore, two ending sites are adiabatically eliminated from the N -site chain. The original system is separated into three independent parts. Two ending-site parts possess two eigenvectors with imaginary eigenvalues $\pm i\gamma$. The third part corresponds to an $(N-2)$ -site single-particle Hermitian SSH chain with open boundary conditions. Although an SSH chain is at total different topological phases for $\mu > 1$ and $\mu < 1$, respectively. However, such an $(N-2)$ -site Hermitian SSH chain is the same as that of the N -site one in the large N limit. In this sense, the coalescing zero mode for $\mu < 1$ represents the same feature as that of $\mu > 1$.

We plot Dirac norm distribution of the coalescing zero mode from Eq. (17) for the Hamiltonian (11) with $N = 30, 22$, and 14, where $P(j) = |\langle j | \psi_{zm} \rangle|$, $j = 1, 2, 3, \dots, N$, as the demonstration of our main result. We see that systems with different size share a common

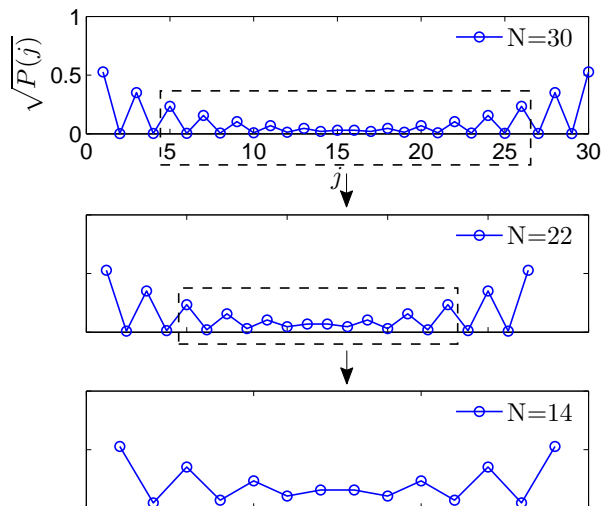


FIG. 2. (Color online) Plots of Dirac norm distribution of the coalescing zero mode from Eq. (17) for the Hamiltonian (11) with $\mu = 1.5$, $\gamma = \mu^{1-N/2}$ for different N . The dashed boxes indicate that the plot for $N = 22$ is a part of $N = 30$, while the plot of $N = 14$ is a part of $N = 22$. Three systems share a common part of wave vector.

part of wave vector. It indicates that one can retrieve the information of the Majorana zero mode in the thermodynamic limit from a small non-Hermitian system. Two degenerate conventional zero modes corresponds to the left and right vectors of the coalescing zero mode.

VI. SUMMARY

In conclusion, we have demonstrated a connection between the topological characterization of an infinite system and the property of a specific small system through a concrete Kitaev model. We have shown that a fine-tuned non-Hermitian \mathcal{PT} -symmetric chemical potential in the finite-size Kitaev ring results in coalescing Majorana zero mode. In particular, such a zero mode in small lattice contains all the information of the conventional degenerate Majorana zero modes in the thermodynamic limit. In addition, the number of edge modes, which includes a pair modes with imaginary eigenvalues, can be a topological invariant to characterize the quantum phase diagram of the corresponding bulk Hermitian system. Although the obtained conclusion is only based on a specific model, it may be a universal feature of the topological system. The underlying mechanism is two fold. Firstly, a single unit cell contains all the information about the bulk system, including the topological feature. Secondly, a finite-size non-Hermitian system, in some way, can be regarded as a sub-system embedded in an infinite system.

Appendix: Evanescent solutions for non-Hermitian SSH chain

1. A. General solution

In this Appendix, we provide the evanescent solutions of the Hamiltonian (11) with $\gamma = \mu^{1-N/2}$ by the Bethe ansatz method. The Bethe ansatz wave function has the form

$$f_l^k = \begin{cases} A_k e^{ikl} + B_k e^{-ikl}, & l = 2j - 1 \\ C_k e^{ikl} + D_k e^{-ikl}, & l = 2j \end{cases}, \quad (\text{A.1})$$

where $j = 1, 2, \dots, N/2$. The explicit form of Schrodinger equation

$$H |\psi_k\rangle = \varepsilon_k |\psi_k\rangle \quad (\text{A.2})$$

is expressed as

$$\begin{cases} f_{m-1}^k - \mu f_{m+1}^k = \varepsilon_k f_m^k \\ f_m^k - \mu f_{m-2}^k = \varepsilon_k f_{m-1}^k \\ f_{m+2}^k - \mu f_m^k = \varepsilon_k f_{m+1}^k \\ f_{m+1}^k - \mu f_{m+3}^k = \varepsilon_k f_{m+2}^k \end{cases} \quad (\text{A.3})$$

in the bulk and

$$\begin{cases} i\gamma f_1^k + f_2^k = \varepsilon_k f_1^k \\ f_{N-1}^k - i\gamma f_N^k = \varepsilon_k f_N^k \end{cases} \quad (\text{A.4})$$

at two ends, where $m = 2j$, $j = 1, 2, 3, \dots, N/2$. From Eq. (A.3) we have the spectrum

$$\varepsilon_k = \pm \sqrt{1 + \mu^2 - \mu(e^{2ik} + e^{-2ik})}, \quad (\text{A.5})$$

and coefficients

$$\frac{B_k}{D_k} = \frac{C_k}{A_k} = e^{-ik} \sqrt{\frac{1 - \mu e^{2ik}}{1 - \mu e^{-2ik}}}. \quad (\text{A.6})$$

Together with Eq. (A.4), we get the equation about k

$$\begin{aligned} & (\varepsilon_k^2 - \gamma^2 - 1) [e^{i(N-2)k} - e^{-i(N-2)k}] \\ & + \mu [e^{i(N-4)k} - e^{-i(N-4)k}] + \mu (\gamma^2 + \varepsilon_k^2) (e^{ikN} - e^{-ikN}) \\ & = 0. \end{aligned} \quad (\text{A.7})$$

In general, the wave function $|\psi_k\rangle$ with real k always represents the scattering vector. Since the real k is bounded by $\pm\pi$, the gap between two branches of eigenvalues ε_k is also bounded by $2|1 - \mu|$.

We are interested in the evanescent wave solution which corresponds to $k = i\kappa$ or $\pi + i\kappa$ (κ is a real number). In this case, Eq. (A.7) becomes

$$\begin{aligned} & (\varepsilon_k^2 - \gamma^2 - 1) \sinh[(N-2)\kappa] + \mu \sinh[(N-4)\kappa] \\ & + \mu (\gamma^2 + \varepsilon_k^2) \sinh(N\kappa) = 0, \end{aligned} \quad (\text{A.8})$$

with eigenvalue

$$\varepsilon_k = \pm \sqrt{1 + \mu^2 - 2\mu \cosh(2\kappa)}. \quad (\text{A.9})$$

At first, it is not hard to find that there are always two solutions

$$\kappa = \pm \frac{1}{2} \ln \mu \quad (\text{A.10})$$

for Eq. (A.8). It leads to $A_k = D_k = 0$ with $\kappa = -\frac{1}{2} \ln \mu$ (or $B_k = C_k = 0$ with $\kappa = \frac{1}{2} \ln \mu$) according to Eq. (A.6). This solution holds for all value of $\mu \neq 1$.

Secondly, in the case of

$$e^{-\kappa N}, e^{-\kappa(N-2)}, e^{-\kappa(N-4)} \ll 1, \quad (\text{A.11})$$

Eq. (A.8) can be reduced to

$$\begin{aligned} (\varepsilon_k^2 - \gamma^2 - 1) e^{\kappa(N-2)} + \mu e^{\kappa(N-4)} \\ + \mu (\gamma^2 + \varepsilon_k^2) e^{\kappa N} = 0, \end{aligned} \quad (\text{A.12})$$

or a more popular form

$$e^{-4\kappa} + \frac{\varepsilon_k^2 - \gamma^2 - 1}{\mu} e^{-2\kappa} + (\gamma^2 + \varepsilon_k^2) = 0. \quad (\text{A.13})$$

Submitting the expression of ε_k into the equation above, it can be approximately reduced to a linear equation for $e^{-2\kappa}$, which has the solution

$$\kappa = \frac{1-N}{2} \ln \mu. \quad (\text{A.14})$$

We note that the relations

$$\begin{cases} \kappa_{\mu=1} = 0 \\ \frac{\partial \kappa}{\partial \mu} < 0 \end{cases}, \quad (\text{A.15})$$

ensure the condition in Eq. (A.11) can be satisfied for the region $\mu < 1$. Then the obtained solution is justified. A similar procedure can be performed in the case of $e^{\kappa N}, e^{\kappa(N-2)}, e^{\kappa(N-4)} \ll 1$. In summary, a pair of solutions with imaginary wave vectors are

$$k = \pm i \frac{1-N}{2} \ln \mu. \quad (\text{A.16})$$

And the corresponding eigenvalues are

$$\varepsilon_{\text{IM}} \approx \pm i \mu^{1-N/2}. \quad (\text{A.17})$$

2. B. Example solution for $N = 6$

We demonstrate the above analysis via exact solutions for $N = 6$ system. Taking $\mu = 2$, we have $\gamma = 1/4$, matrix h_{SSH} is expressed explicitly as

$$M_1 = \begin{pmatrix} i/4 & 1 & 0 & 0 & 0 & 0 \\ 1 & 0 & 2 & 0 & 0 & 0 \\ 0 & 2 & 0 & 1 & 0 & 0 \\ 0 & 0 & 1 & 0 & 2 & 0 \\ 0 & 0 & 0 & 2 & 0 & 1 \\ 0 & 0 & 0 & 0 & 1 & -i/4 \end{pmatrix}. \quad (\text{A.18})$$

The eigenvalues are

$$\begin{aligned} \varepsilon_1 = \varepsilon_2 = 0, \\ \varepsilon_3 = -\varepsilon_4 = \frac{1}{8} \sqrt{350 + 2\sqrt{3553}}, \\ \varepsilon_5 = -\varepsilon_6 = \frac{1}{8} \sqrt{350 - 2\sqrt{3553}}, \end{aligned} \quad (\text{A.19})$$

which are all real. Two zero-mode eigen vectors are identical, i.e.,

$$\phi_1 = \phi_2 = (4i, 1, -2i, -2, i, 4), \quad (\text{A.20})$$

which has zero biorthogonal norm.

Taking $\mu = 1/2$, we have $\gamma = 4$, matrix h_{SSH} is expressed explicitly as

$$M_2 = \begin{pmatrix} i4 & 1 & 0 & 0 & 0 & 0 \\ 1 & 0 & 1/2 & 0 & 0 & 0 \\ 0 & 1/2 & 0 & 1 & 0 & 0 \\ 0 & 0 & 1 & 0 & 1/2 & 0 \\ 0 & 0 & 0 & 1/2 & 0 & 1 \\ 0 & 0 & 0 & 0 & 1 & -i4 \end{pmatrix}, \quad (\text{A.21})$$

The eigenvalues are

$$\begin{aligned} \varepsilon_1 = \varepsilon_2 = 0, \\ \varepsilon_3 = -\varepsilon_4 = \frac{i}{2} \sqrt{2\sqrt{238} + 25}, \\ \varepsilon_5 = -\varepsilon_6 = \frac{1}{2} \sqrt{2\sqrt{238} - 25}, \end{aligned} \quad (\text{A.22})$$

which contains a pair of imaginary numbers. Two zero-mode eigen vectors are identical, i.e.

$$\phi_1 = \phi_2 = (i, 4, -2i, -2, 4i, 1), \quad (\text{A.23})$$

which has zero biorthogonal norm. In both two cases, vectors ϕ_1, ϕ_2 are not normalized.

ACKNOWLEDGMENTS

We acknowledge the support of the CNSF (Grant No. 11374163).

-
- [1] M. Z. Hasan, and C. L. Kane, *Rev. Mod. Phys.* **82**, 3045 (2010).
- [2] X. L. Qi, and S. C. Zhang, *Rev. Mod. Phys.* **83**, 1057 (2011).
- [3] C. K. Chiu, J. C. Y. Teo, A. P. Schnyder, and S. Ryu, *Rev. Mod. Phys.* **88**, 035005 (2016).
- [4] H. M. Weng, R. Yu, X. Hu, X. Dai, and Z. Fang, *Adv. Phys.* **64**, 227 (2015).
- [5] J. K. Asboth, L. Oroszlany, and A. Palyi, *A short course on topological insulators: Band-structure topology and edge states in one and two dimensions* (Springer, 2016).
- [6] L. Jin and Z. Song, *Phys. Rev. A* **81**, 032109 (2010); *Phys. Rev. A* **83**, 062118 (2011); *J. Phys. A: Math. Theor.* **44**, 375304 (2011).
- [7] A. Y. Kitaev, *Physics-Uspokhi* **44**, 131 (2001).
- [8] V. Mourik, K. Zuo, S. M. Frolov, S. R. Plissard, E. P. A. M. Bakkers, and L. P. Kouwenhoven, *Science* **336**, 1003 (2012).
- [9] L. P. Rokhinson, X. Liu, and J. K. Furdyna, *Nat. Phys.* **8**, 795 (2012).
- [10] A. Das, Y. Ronen, Y. Most, Y. Oreg, M. Heiblum, and H. Shtrikman, *Nat. Phys.* **8**, 887 (2012).
- [11] A. D. K. Finck, D. J. Van Harlingen, P. K. Mohseni, K. Jung, and X. Li, *Phys. Rev. Lett.* **110**, 126406 (2013).
- [12] A. Banerjee, C. A. Bridges, J. Q. Yan, et al., *Nature Materials*. **15**, 733 (2016).
- [13] C. Li, S. Lin, G. Zhang, and Z. Song, arXiv:1704.04990.
- [14] S. Lin, G. Zhang, C. Li, and Z. Song, *Sci. Rep.* **6**, 31953 (2016); G. Zhang, C. Li, and Z. Song, *Sci. Rep.* **7**, 8176 (2017).
- [15] S. Lin, X. Z. Zhang, C. Li, and Z. Song, *Phys. Rev. A* **94**, 042133 (2016).
- [16] M. Klett, H. Cartarius, D. Dast, J. Main, and G. Wunner, *Phys. Rev. A* **95**, 053626 (2017).
- [17] A. Mostafazadeh, *J. Math. Phys.* **43**, 205 (2002).
- [18] L. Jin and Z. Song, *Phys. Rev. A* **80**, 052107 (2009).
- [19] H. Schomerus, *Opt. Lett.* **38**, 1912–1914 (2013).
- [20] C. Poli, M. Bellec, U. Kuhl, F. Mortessagne, and H. Schomerus, *Nat. Commun.* **6**, 6710 (2015).
- [21] J. M. Zeuner, et al., *Phys. Rev. Lett.* **115**, 040402 (2015).
- [22] S. Weimann, et al., *Nat. Mater.* **16**, 433–438 (2017).